

Recyclable conductive nanoclay for direct in-situ printing flexible electronics

Pengcheng Wu,^{a,b} Zhenwei Wang,^{a,b} Xinhua Yao,^{*a,b} Jianzhong Fu^{a,b} and Yong He^{*a,b,c}

^aState Key Laboratory of Fluid Power and Mechatronic Systems, School of Mechanical Engineering, Zhejiang University, Hangzhou 310027, China

^bKey Laboratory of 3D Printing Process and Equipment of Zhejiang Province, School of Mechanical Engineering, Zhejiang University, Hangzhou 310027, China

^cKey Laboratory of Materials Processing and Mold, Zhengzhou University, Zhengzhou 450002, China

** Correspondence to: Yong He, e-mail: yongqin@zju.edu.cn*

Xinhua Yao, e-mail: yaoxinhua@zju.edu.cn

Supplementary Text

Figure S1. Three states in the stirring process of nanoclay and liquid metal.

Figure S2. Morphology of conductive nanoclay on the stamp.

Figure S3. Nanoclay aggregates at the interface of the conductive trace and PDMS substrate.

Figure S4. Exposed nanoclay aggregates of conductive trace by stamp printing.

Figure S5. The energy dispersive spectrometer (EDS) mapping of the interface between conductive trace and PDMS substrate.

Figure S6. High-precision circuit based on stamp printing.

Figure S7. EDS mapping of conductive nanoclay internal crosssection and the content of elements (Ga, In, Si, and Mg) on it.

Figure S8. The damage mitigation ability of conductive nanoclay.

Figure S9. The working process of vacuum-on switch.

Figure S10. The states of the printed circuit during the bending of the wrist.

Figure S11. Conductivity of conductive nanoclay with different mass ratios of liquid metal and nanoclay.

Figure S12. The rheological properties of the conductive nanoclay with different mass ratios of liquid metal and nanoclay.

Figure S13. Device and principle of adhesion test of conductive nanoclay.

Figure S14. The results of the adhesion experiment of conductive nanoclay.

Figure S15. The mass changes of silicone elastomer substrates with different conductive nanoclays after pressing.

Figure S16. Scraping experiment to conductive nanoclay on silicone elastomer substrate.

Figure S17. Recyclable flexible electronics.

Figure S18. Morphology of nanoclay before and after mixing with liquid metal.

Movie S1. Tensile experiment of the repaired circuit.

Movie S2. The Vacuum-on switch experiment.



Figure S1. Three states in the stirring process of nanoclay and liquid metal: initial state(A), intermediate state(B) and final state(C).

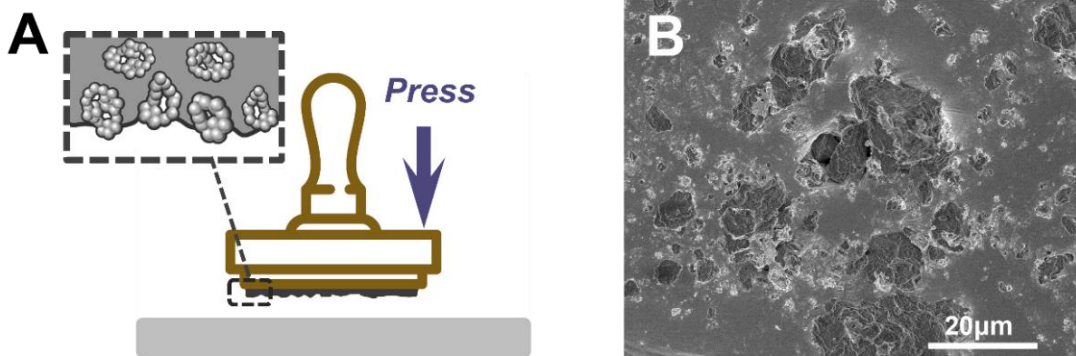


Figure S2. Morphology of conductive nanoclay on the stamp. Conductive nanoclay on the stamp exhibits a rough surface (A), and the exposed nanoclay is observed through the SEM image(B), which directly contacts the substrate material and forms fulcrums for reliable conductive paths in the subsequent stamp printing process.

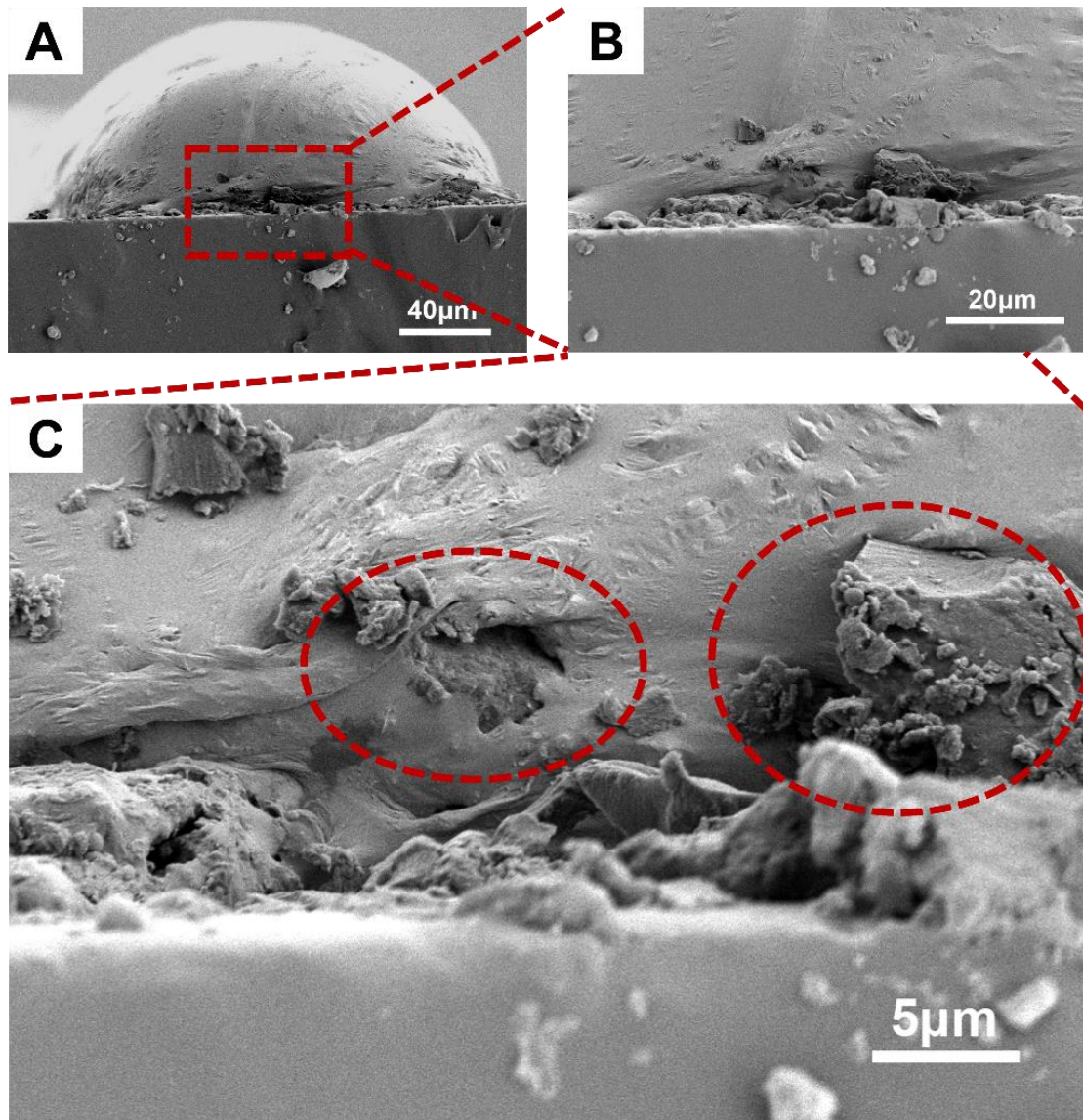


Figure S3. Nanoclay aggregates at the interface of the conductive trace and PDMS substrate.

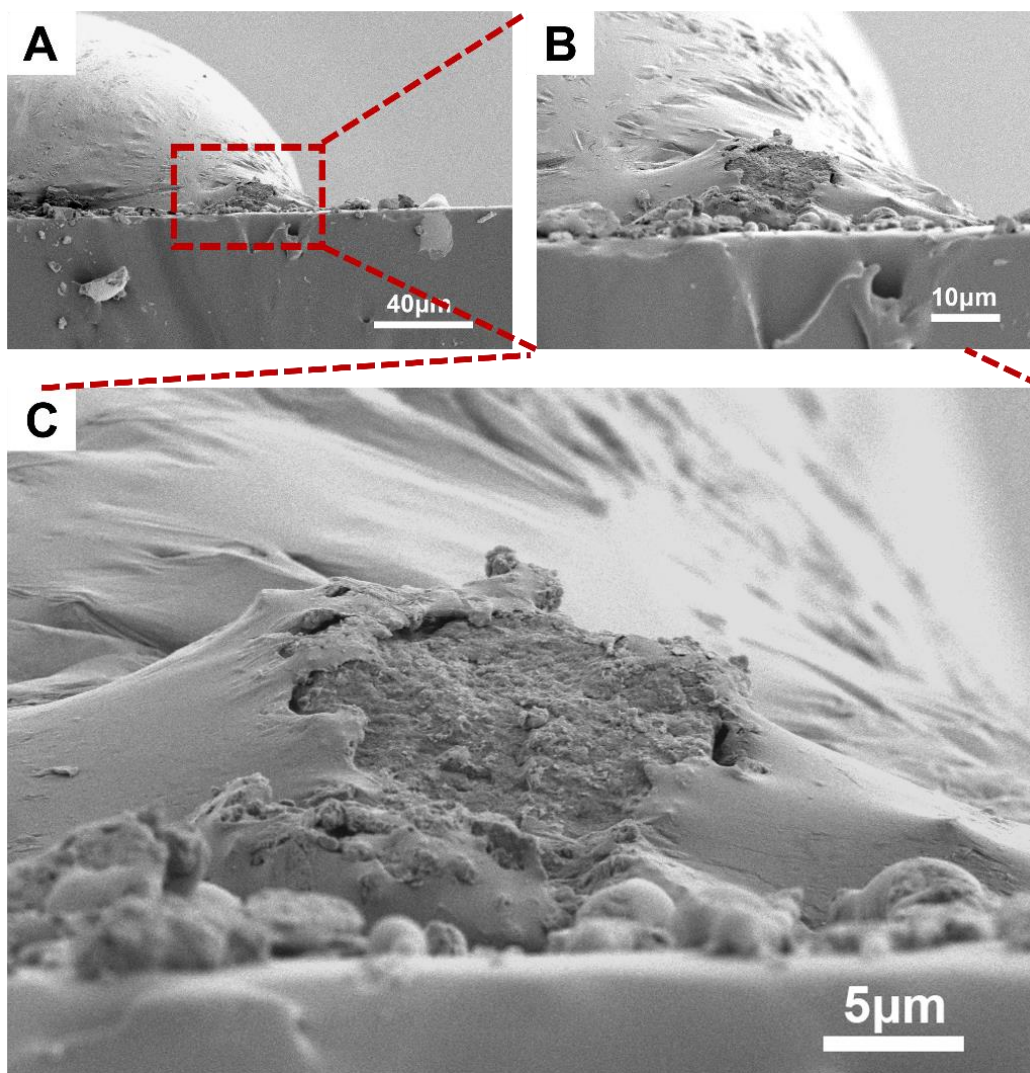


Figure S4. Exposed nanoclay aggregates of conductive trace by stamp printing.

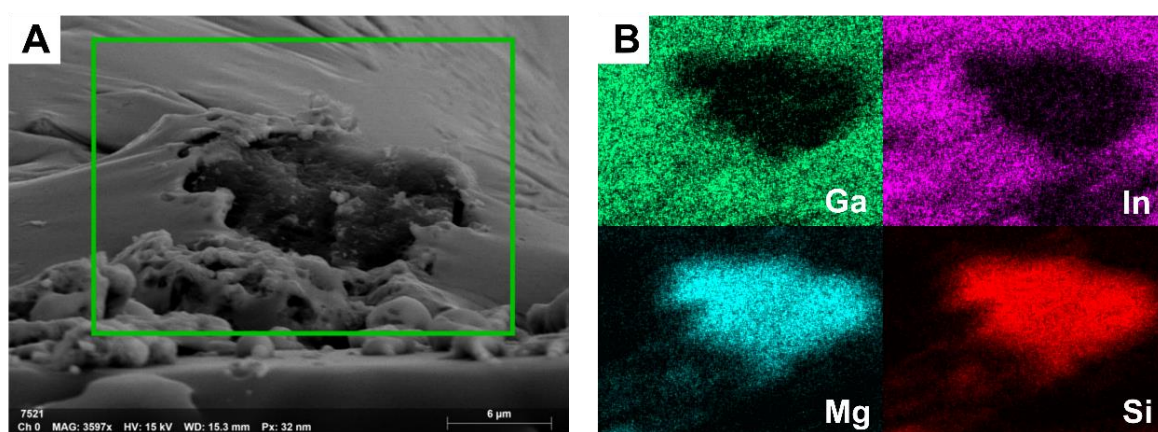


Figure S5. The energy dispersive spectrometer (EDS) mapping of the interface between conductive trace and PDMS substrate.

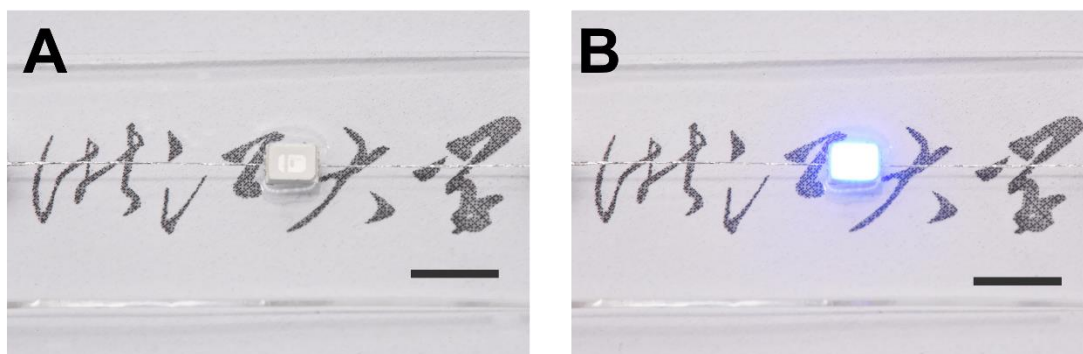


Figure S6. High-precision circuit based on stamp printing. The scale bar is 5mm.

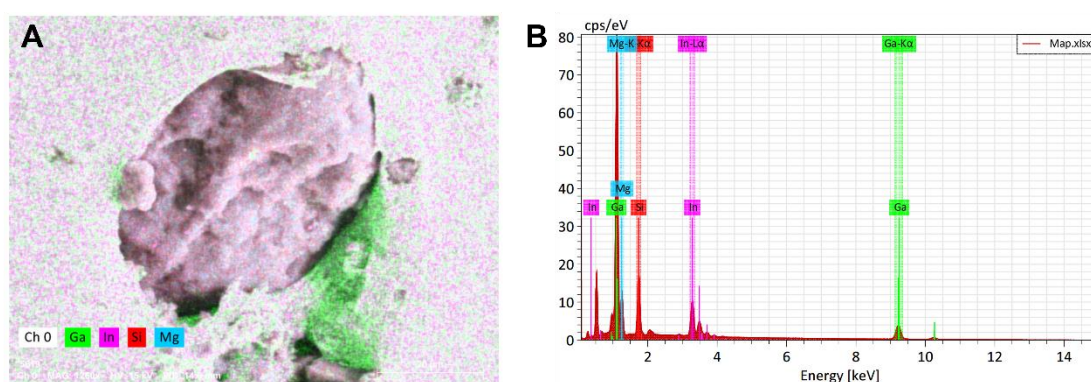


Figure S7. EDS mapping of conductive nanoclay internal crosssection and the content of elements (Ga, In, Si, and Mg) on it.

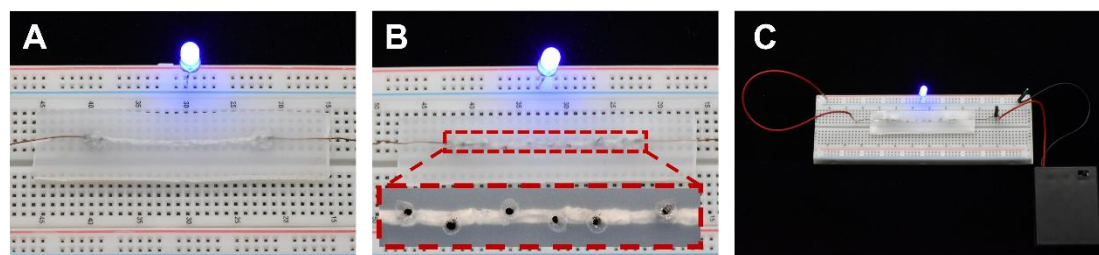


Figure S8. The damage mitigation ability of conductive nanoclay. (A) The initial state of the conductive path based on conductive nanoclay and stamp printing. (B) Conductive path after 6 hole punches. (C) Optical image of the complete circuit.

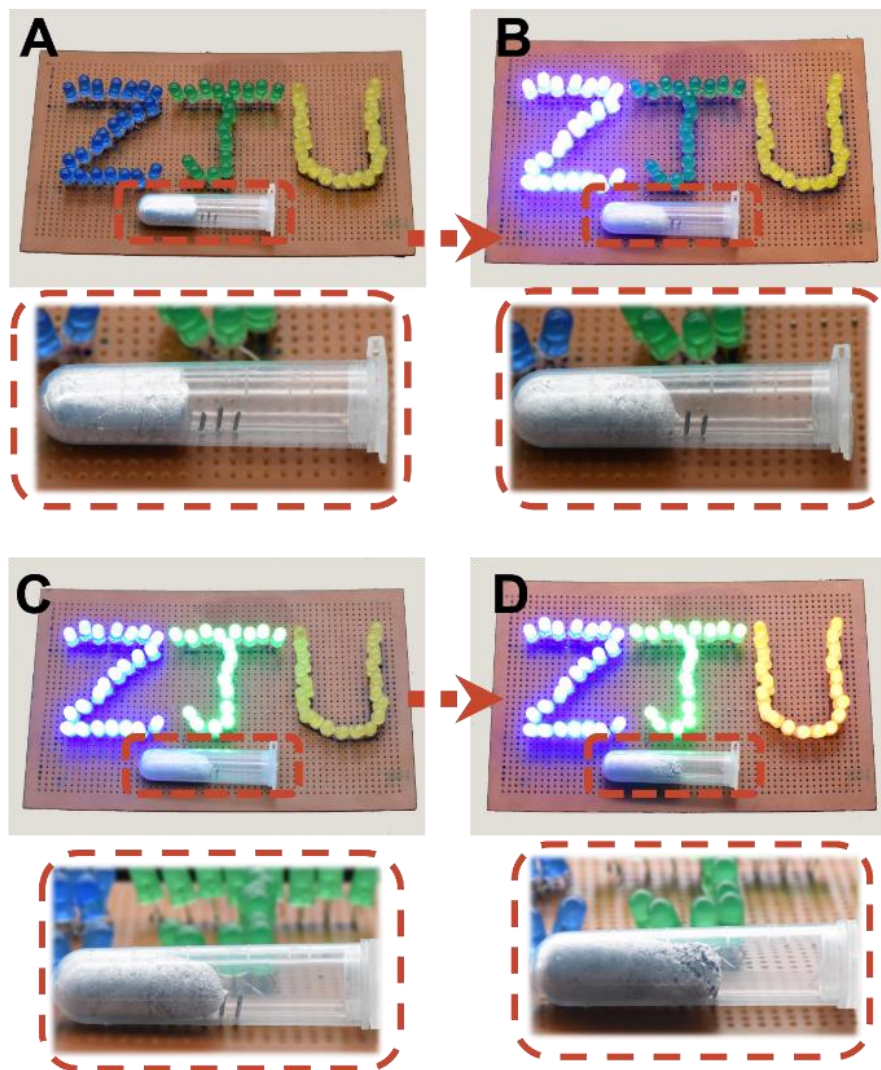


Figure S9. The working process of vacuum-on switch.

The vacuum-on switch shown in Figure S9 utilizes the vacuum growth performance of conductive nanoclay to light up three LED arrays. During this process, the electrode will inevitably damage the structure of the grown conductive nanoclay, making it difficult to completely restore to the initial state when pressure is restored, so the vacuum-on switch shown in Figure S9 is irreversible. However, when the vacuum switches are actually applied in some special occasions such as outer space, the on/off state of each logical circuit must be controlled by an independent vacuum-on switch, which means that the conductive nanoclay in the switch only needs to be in contact with the electrode without overgrowth, so that the structure of the conductive nanoclay will not be destroyed, and can be used repeatedly with no residue on the electrode. Moreover, when the air pressure is restored, conductive nanoclay residue on the electrode is negligible because the electrode is relatively small. Therefore, there will be no short circuit in the normal use of the vacuum switches.

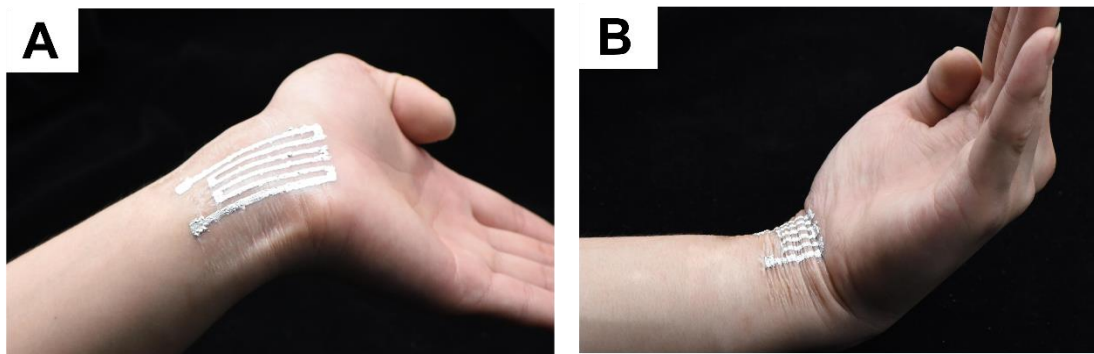


Figure S10. The states of the printed circuit during the bending of the wrist. (A)The outward bending of the wrist. (B)The inward bending of the wrist.

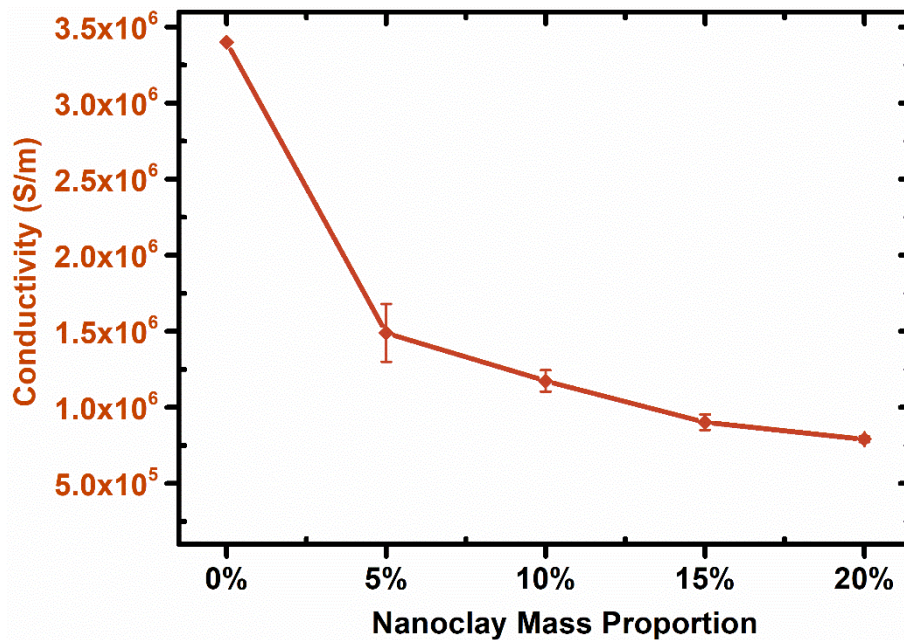


Figure S11. Conductivity of conductive nanoclay with different mass ratios of liquid metal and nanoclay. The error bars are the standard deviation.

We conducted electrical conductivity tests on conductive nanoclays with different mass proportions of nanoclay: as the content of nanoclay increases (5%-20%), the electrical conductivity decreases, but the electrical conductivity ($\sim 10^6$ S/m) can still meet the requirements of most conductors (Figure S11). Flow curves of conductive nanoclays with different mass proportions of nanoclay were shown in Figure R3-7. These liquids show a drop in viscosity at high shear rates and possess low viscosity at high EGaIn content.

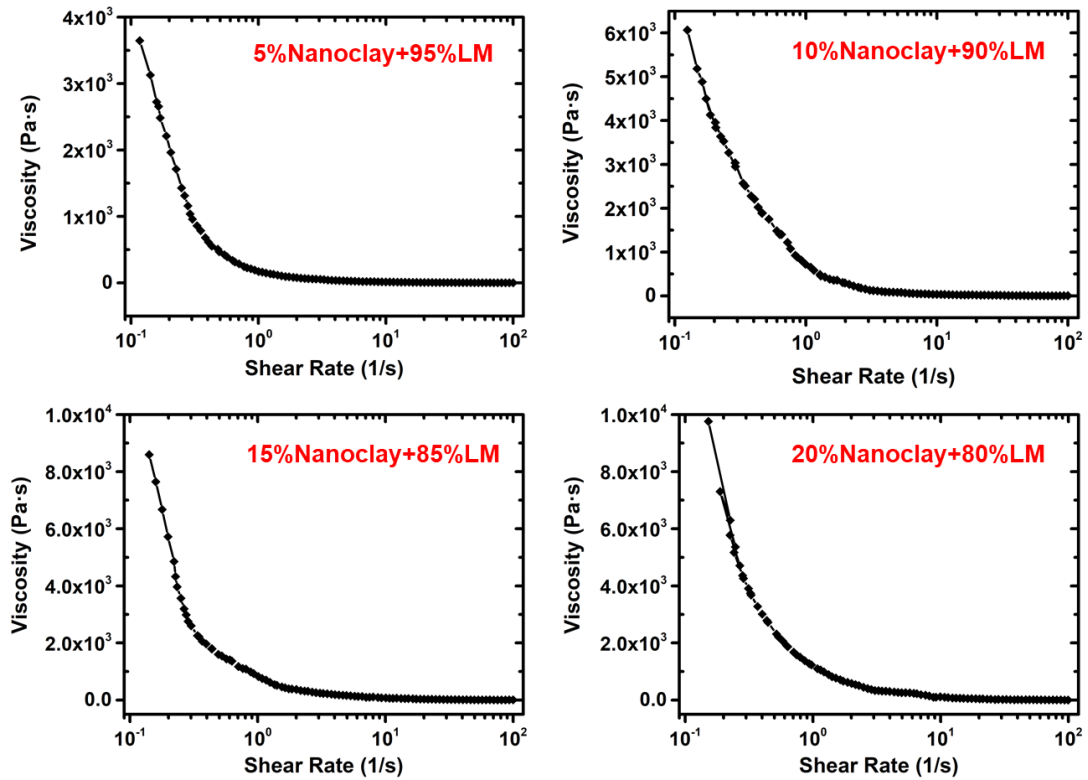


Figure S12. The rheological properties of the conductive nanoclay with different mass ratios of liquid metal and nanoclay.

All rheological properties curves of conductive nanoclay were obtained by a rotational rheometer (HAAKE RheoStress 6000, Thermo Fisher Scientific, USA) at 25 °C. The distance between the upper and lower geometries was 1 mm. Viscosity measurements were obtained in the shear rate ranging of 0.1-100 s⁻¹ during the 120s.

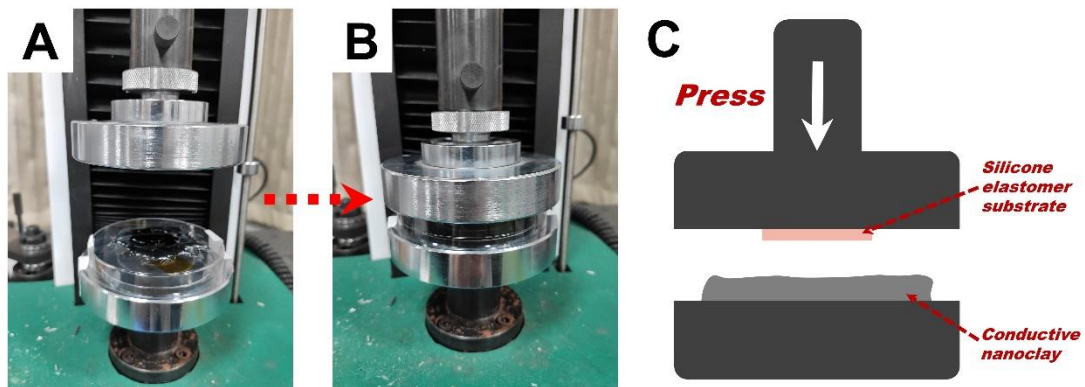


Figure S13. Device and principle of adhesion test of conductive nanoclay.

In order to verify that the conductive nanoclay has better adhesion performance, we designed an adhesion test experiment. We attached a 2cm×2cm silicone elastomer substrate to the vertical moving platform, and then pressed it on the conductive nanoclay with a pressure of 5N, and held it on the conductive nanoclay for 30s, and then the platform was lifted to test the mass change of silicone elastomer substrate to characterize the adhesion performance of the conductive nanoclay to the silicone

elastomer substrate. The test device and test principle are shown in Figure S13. We set up 5 groups of experiments, in which pure liquid metal is the control group, and the mass proportions of nanoclay in the other groups are 5%, 10%, 15%, and 20%, respectively.

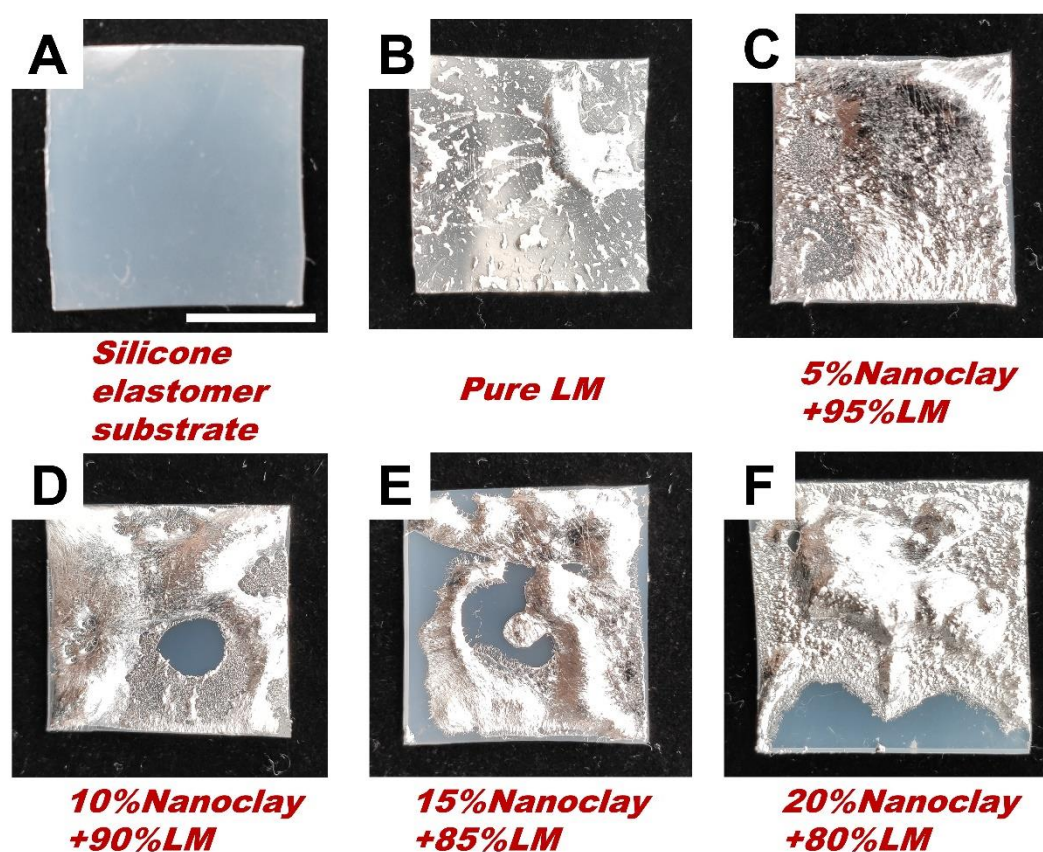


Figure S14. The results of the adhesion experiment of conductive nanoclay. The scale bar is 1cm.

The results of the adhesion experiment of conductive nanoclay are shown in Figure S14. The adhesion of pure liquid metal to the substrate is the worst. The adhesion of 5% nanoclay + 95% LM conductive nanoclay to the substrate is significantly better than that of pure liquid metal. As the content of nanoclay increases, it seems that the adhesion performance of conductive nanoclay decreases (5%-20%, the adhesion area of conductive nanoclay on the substrate decreases). In fact, as the content of nanoclay increases, we have found that conductive nanoclays tend to be more solid in nature, and the deformation is very small under the same force. It is difficult to ensure absolute flatness on the surface of conductive nanoclays as inkpads, and therefore the adhesion area on the substrate decreases as the hardness of the conductive nanoclay increases. The mass changes of silicone elastomer substrates with different conductive nanoclays are shown in Figure S15.

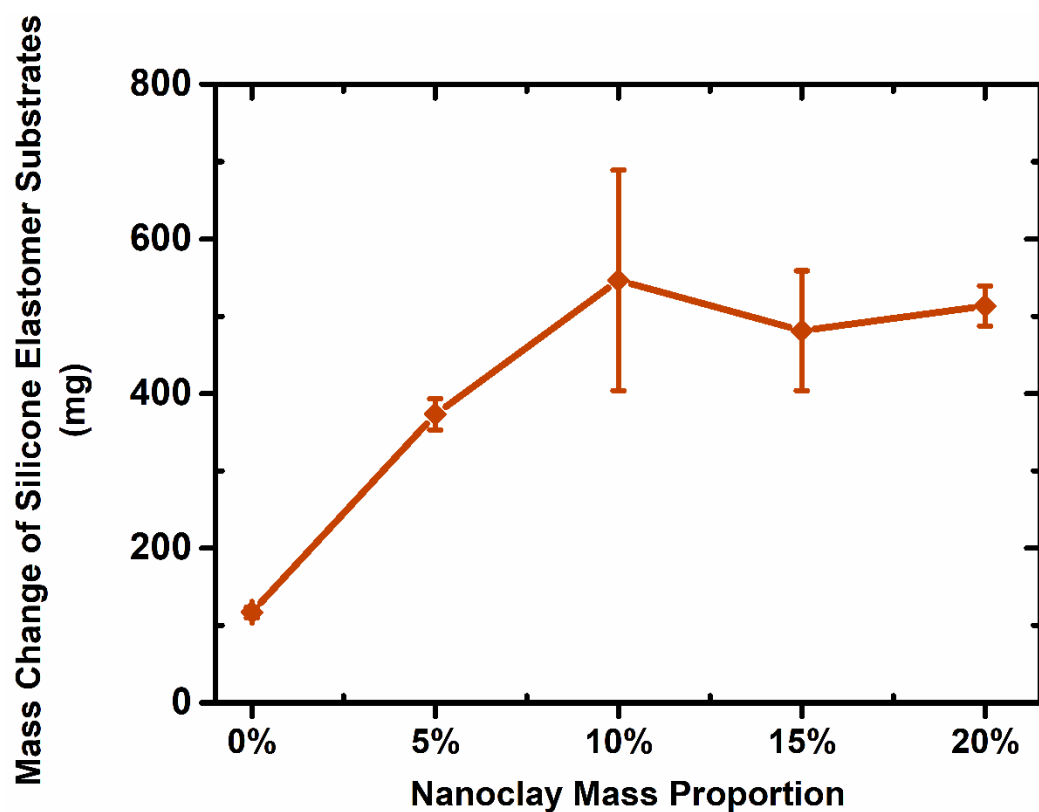


Figure S15. The mass changes of silicone elastomer substrates with different conductive nanoclays after pressing.



Figure S16. Scraping experiment to conductive nanoclay on silicone elastomer substrate. The scale bar is 1cm.

Then we tried to scrape away the conductive nanoclay adhered to the silicone elastomer substrate. We can clearly find that there are obvious connections between the conductive nanoclay and the substrate, which can further prove the superior adhesion of the conductive nanoclay to the silicone elastomer substrate (Figure S16).

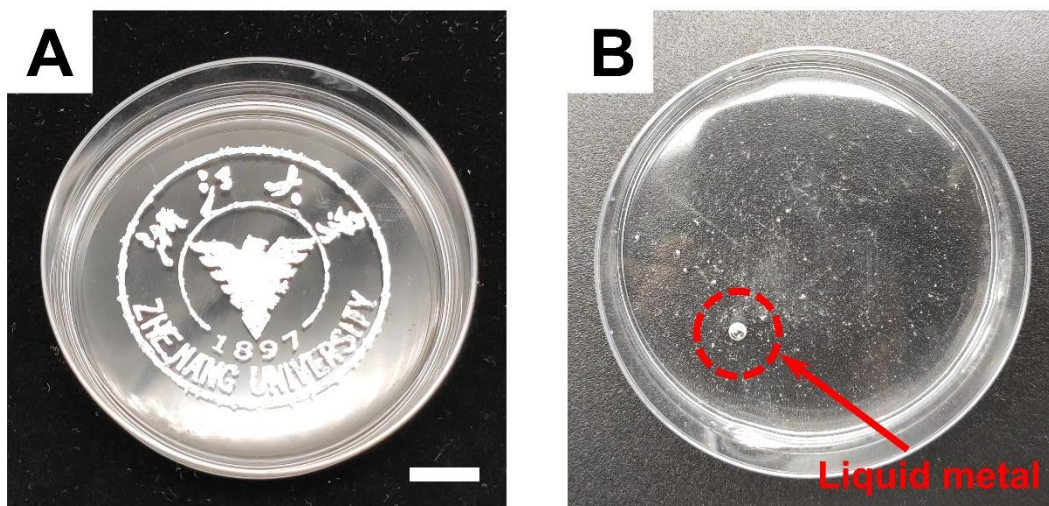


Figure S17. Recyclable flexible electronics. The scale bar is 1 cm.

Electronic products have brought huge improvements to people's lives, but the increasing electronic waste has become large sources of environmental pollution, most of which is hard to degrade and cannot be recycled. In order to verify the recyclability of the flexible electronics using conductive nanoclay, we printed the school badge of Zhejiang University on the PDMS substrate, then poured 2M HCl into petri dish, stirred the solution with a glass rod, we could recover the liquid metal, and the PDMS substrate can be reused (Figure S17).

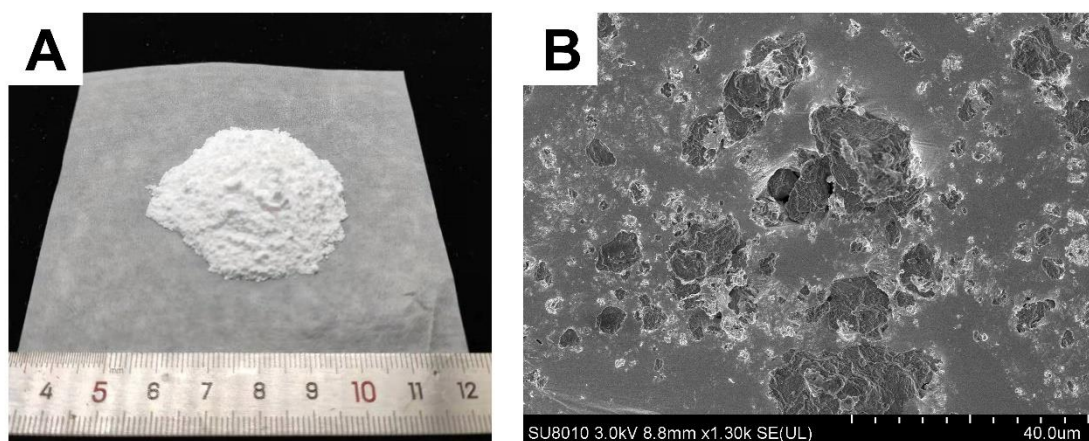


Figure S18. Morphology of nanoclay before and after mixing with liquid metal. (A) 4g nanoclay. (B) SEM image of conductive nanoclay (20% nanoclay + 80% LM).